ENCIT 2018

ABCM Associação Brasileira de Engenharia e Ciências Mecânicas

17th Brazilian Congress of Thermal Sciences and Engineering
November 25th-28th, 2018, Águas de Lindóia, SP, Brazil

ENCIT-2018-0680
NUMERICAL EVALUATION OF MENTER'S SST-CC MODEL FOR AN ANNULAR-SECTOR DUCT ROTATING IN PARALLEL MODE

Vinicius Daroz
Admilson T. Franco
Eduardo M. Germer
Research Center for Rheology and Non Newtonian Fluids - Federal University of Technology - Curitiba - Parana - Brazil
vdaroz@utfpr.edu.br, admilson@utpr.edu.br, eduardomg@utfpr.edu.br
Diogo B. Pitz
Department of Mechanical Engineering Sciences - University of Surrey - United Kingdom
diogopitz@gmail.com

Abstract. *Turbulence models based on the eddy-viscosity are, by construction, insensitive to rotation, curvature and anisotropy effects. To incorporate their contributions to the flow dynamics, ad-hoc corrections are usually implemented in the model equations. The correction method used in this study, considering Menter's SST as base model, consists of multiplying the turbulence kinetic energy production term by a correction factor. The SST model with curvature correction (SST-CC), was tested against large-eddy simulation (LES) results for an annular-sector duct rotating in parallel mode. The model assertability was inferred by comparing first-order mean quantities. The corrected model was able to incorporate rotational effects and the results for the velocity field agreed well with those obtained with LES. The plain SST model, besides being insensitive to rotation, also delivered qualitatively good results.*

Keywords: *LES, SST, SST-CC, curvature correction, annular-sector*

1. INTRODUCTION

Turbulent flows in the presence of curvature and rotation are common in many engineering applications such as turbomachinery, heat exchangers, electric generators, to name a few examples. Rotation effects induced by Coriollis or centrifugal forces are not accounted for in standard Reynolds-averaged Navier-Stokes (RANS) turbulence models based on the eddy viscosity hypothesis. Their native formulation is also insensitive to curvature effects requiring ad-hoc corrections (Arolla and Durbin, 2013).

Despite the fast advances in computing power and consequently more use of turbulence-resolving approaches, RANS-based models still remain the widely used tool for turbulent flow computation. Menter's shear-stress transport model (Menter, 1992) was proposed as a model that gathered the best characteristics of Wilcox $k-\omega$ (Wilcox, 1988) and Patankar's $k-\epsilon$ model (Patankar *et al.*, 1975) with great success in aerodynamic and general-purpose industrial applications (Menter *et al.*, 2003). By using a blending function, the model is able to switch from $k-\omega$, for near-wall regions, to $k-\epsilon$ for free stream regions. By doing that, it predicts the behaviour of both internal and external turbulent flows quite well with fair CPU time usage.

Nevertheless, scalar turbulence closure models are derived from transport equations for scalar quantities. By definition, they do not respond appropriately to directional forces, such as those arising from system rotation and streamline curvature, which are known to affect individual components of the Reynolds stress tensor. A scalar formula does not distinguish directional components of Reynolds stresses, so the correct phenomenology is inherently absent (Durbin, 2011). To deal with this issue, Patankar et al., 1975 proposed a correction correlation which was first applied to the Sparlart-Allmaras one-equation model (Spalart and Shur, 1997). The method consisted of multiplying the production term by a correction function which accounted for streamline curvature and system rotation effects. The idea was then adapted to the SST model, correcting the production terms in both k and ω transport equations, to create the SST-CC model which showed great improvements in comparison with the original SST (Smirnov and Menter, 2009).

More recently, Arolla and Durbin (2013) proposed a new method as they pointed out that correcting the production term without altering the turbulent viscosity in the momentum equation is physically inconsistent. Their approach is based on the bifurcation analysis of Reynolds Stress models for rotating homogeneous shear flows. Since the SST model does not show such bifurcation behaviour, the proposed correction mimics this effect by correcting the turbulent viscosity coefficient.

In order to test the model on predicting complex turbulent flows, in the present study, the fully developed turbulent flow within an annular-sector duct rotating in parallel mode is solved with the aid of a commercial CFD code. The results obtained with both SST and SST-CC models are compared to LES results obtained with the dynamic Smagorinsky-Lilly model.

2. MATHEMATICAL MODELLING

The governing equations are derived for a Newtonian incompressible fluid. Gravity is neglected and the duct walls are considered to be smooth and impermeable. The problem geometry is represented in Fig. 1. The annular-sector duct is characterized by the outer radius R, the radii ratio η, the apex angle α and the height H. The gorvening equations are derived for a rotating frame of reference, which rotates about the z-axis with rotational speed ω. The flow is considered to be fully developed so that periodic boundary conditions are applied in the streamwise direction.

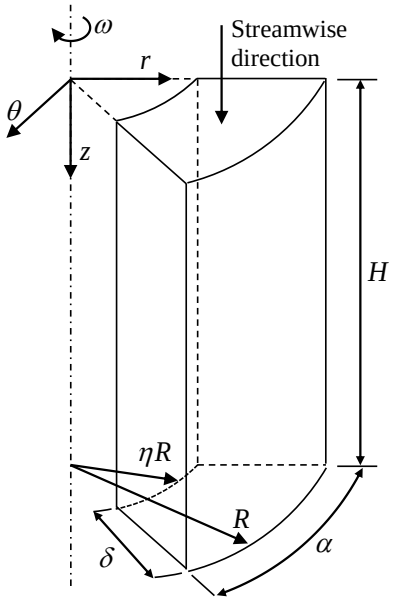

Figure 1: Geometric configuration of the problem

If the time-averaging and space-filtering operators are taken to be represented by:

$$\overline{f} = f - f', \tag{1}$$

where f denotes any flow quantity, $\overline{f}$ its space-filtered or time-averaged parcel and f' the non-filtered or fluctuating parcel, the continuity and momentum equations become respectively:

$$\nabla \cdot \overline{\mathbf{u}} = 0 \tag{2}$$

$$\frac{\partial \overline{\mathbf{u}}}{\partial t} + (\overline{\mathbf{u}} \cdot \nabla)\,\overline{\mathbf{u}} + 2\boldsymbol{\Omega} \times \overline{\mathbf{u}} = -\frac{1}{\rho}\nabla \overline{P} + \frac{1}{\rho}\nabla\left(\overline{\mathbf{T}} - \mathbf{T}^{\mathrm{M}}\right) \tag{3}$$

In Eq. (2) and (3), $\mathbf{u}$ is the velocity vector, $\boldsymbol{\Omega}$ is the rotation vector, $\overline{P}$ is the modified pressure (the centrifugal force and the isotropic part of $\mathbf{T}^{\mathrm{M}}$ are added to the pressure term), ρ is the fluid density and $\mathbf{T}$ is the viscous-stress tensor. The term $\mathbf{T}^{\mathrm{M}}$ represents the subgrid-stress tensor for the LES formulation and the Reynolds stress tensor for the RANS formulation. For both LES and RANS formulations, $\mathbf{T}^{\mathrm{M}}$ is dealt with based on the Boussinesq hypothesis for the eddy-viscosity (ν_t). The equations for $\mathbf{T}^{\mathrm{M}} = \tau_{ij}^{\mathrm{M}}$ and ν_t are:

$$\tau_{ij}^{\mathrm{M}} - \frac{1}{3}\delta_{ij}\tau_{ij}^{\mathrm{M}} = \nu_t \overline{S}_{ij} \tag{4}$$

$$\nu_t = \begin{cases} kT & \text{if SSTKO} \\ C_s^2 V^{2/3} \left|\overline{S}\right| & \text{if DynSMG} \end{cases} \tag{5}$$

where the subscripts ij represent the summation notation and δ_{ij} is the Kronecker delta. The derivation of closure relations to obtain ν_t in Eq. (5) is what differentiates the variety of eddy-viscosity models. For the SSTKO, ν_t is obtained from the product of T, the turbulent time scale, and k, the turbulent kinetic energy. In the case of the DynSMG model, C_s is the dynamic constant of the model, V the cell volume and $\overline{S}$ the resolved strain-rate tensor modulus.

2.1 SST and curvature correction formulation

In order to obtain ν_t in Eq. (5), it is necessary to derive closure relations to the involved quantities. The turbulent time scale T is defined according to Eq. (6).

$$T = \min\left(\frac{\alpha^*}{\omega}, \frac{\mathrm{a}_1}{SF_2}\right) \tag{6}$$

In Eq. (6), $\alpha^* = 1$, $F2$ is a blending function calculated according to Eq. (7), ω is the specific dissipation rate, $\mathrm{a}_1 = 0.31$ and S the time-averaged strain-rate tensor modulus. Menter's original model (Menter, 1992) uses the modulus of the vorticity tensor rather than S. This slight modification extends the applicability of the model beyond aerodynamic applications. Furthermore, Durbin's realizability constraint is used instead of Menter's proposal (Siemens, 2017).

$$F_2 = \tanh\left[\left(\max\left(\frac{2\sqrt{k}}{\beta^*\omega d}, \frac{500\nu}{d^2\omega}\right)\right)^2\right] \tag{7}$$

In Eq. (7), ν is the fluid kinematic viscosity, d is the distance to the wall and β^* is a model coefficient given by:

$$\beta^* = F_1\beta_1^* + (1 - F_1)\beta_2^* \tag{8}$$

in which $\beta_1^* = \beta_2^* = 0.09$ and F_1 is another blending function defined as:

$$F_1 = \tanh\left(\left[\min\left(\max\left(\frac{\sqrt{k}}{0.09\omega d}, \frac{500\nu}{d^2\omega}\right), \frac{2k}{d^2\mathrm{CD}_{k\omega}}\right)\right]^4\right) \tag{9}$$

where $\mathrm{CD}_{k\omega}$ is the cross diffusion coefficient given in Eq. (10).

$$\mathrm{CD}_{k\omega} = \max\left(\frac{1}{\omega}\nabla k \cdot \nabla\omega, 10^{-20}\right) \tag{10}$$

The transport equations for k and ω are presented in equations (11) and (12).

$$\frac{\partial}{\partial t}(\rho k) + \nabla\cdot(\rho k\overline{\mathbf{v}}) = \nabla\cdot\left[(\mu + \sigma_k\mu_t)\nabla k\right] + P_k - \rho\beta^*\omega k \tag{11}$$

$$\frac{\partial}{\partial t}(\rho\omega) + \nabla\cdot(\rho\omega\overline{\mathbf{v}}) = \nabla\cdot\left[(\mu + \sigma_\omega\mu_t)\nabla\omega\right] + P_\omega - \rho\beta\omega^2 \tag{12}$$

where:

$$\sigma_k = F_1\sigma_{k_1} + (1 - F_1)\,\sigma_{k_2} \tag{13}$$

$$\sigma_\omega = F_1\sigma_{\omega_1} + (1 - F_1)\,\sigma_{\omega_2} \tag{14}$$

where $\sigma_{k_1} = 0.85$, $\sigma_{k_2} = 1$, $\sigma_{\omega_1} = 0.5$ and $\sigma_{\omega_2} = 0.856$ are model constants.

Equation (11) is insensitive, by construction, to stabilizing and destabilizing effects usually associated with strong (streamline) curvature and frame-rotation (Siemens, 2017). The curvature correction factor f_c, comes into play to alter the turbulent kinetic energy production term (Eq. (15)) according to the local rotation and vorticity rates.

$$P_k = \mu_t f_c S^2 \tag{15}$$

in which the correction factor is given by:

$$f_c = \min\left(C_{\max}, \frac{1}{c_{r1}\left(|\eta| - \eta\right) + \sqrt{1 - \min\left(c_{r2}\eta, 0.99\right)}}\right) \tag{16}$$

where $C_{\max} = 1.25$ (Upper limit), $c_{r1} = 0.04645$, $c_{r2} = 0.25$. The dimensionless velocity gradient invariant η is obtained from:

$$\eta = T^2\left(\mathbf{S} : \mathbf{S} - \mathbf{W} : \mathbf{W}\right). \tag{17}$$

The time scale T is limited in order to have the correct near-wall asymptotic behaviour, $T = \max\left(T_1, T_3\right)$, where:

$$T_1 = \frac{1}{\beta^* \omega} \qquad T_2 = 6\sqrt{\frac{\nu}{\beta^* k \omega}} \quad T_3 = \left(T_1^{1.625} T_2\right)^{\frac{1}{1.625+1}} \tag{18}$$

The strain-rate tensor $\mathbf{S}$ and the absolute rotation-rate tensor $\mathbf{W}$ are calculated as:

$$\mathbf{S} = \frac{1}{2}\left(\nabla\overline{\mathbf{v}} + \nabla\overline{\mathbf{v}}^T\right) \tag{19}$$

$$\mathbf{W} = \mathbf{W}^l + \mathbf{W}^f + \left(C_{ct} - 1\right)\mathbf{W}^S \tag{20}$$

where $\mathbf{W}^l$, $\mathbf{W}^f$ and $\mathbf{W}^S$, defined in Eqs. (21), (22) and (23) respectively, are the contributions due to vorticity computed in the local reference frame, vorticity computed in the rotating reference frame and streamline curvature, respectively. C_{ct} is a model constant and assumes the value $C_{ct} = 2$.

$$\mathbf{W}^l = \frac{1}{2}\left(\nabla\overline{\mathbf{v}} + \nabla\overline{\mathbf{v}}^T\right) \tag{21}$$

$$\mathbf{W}^f = \mathbf{E} \cdot \omega^f \tag{22}$$

$$\mathbf{W}^S = \mathbf{W}^f - \mathbf{E} \cdot \left(\mathbf{A}^{-1} \cdot \omega\right) \tag{23}$$

In Eqs. 22 and 23, $\mathbf{E}$ is the Levi-Civita tensor (also know as the three-dimensional permutation tensor).

$$\mathbf{A} = \mathbf{I} - \frac{3\mathbf{S}^2}{2\mathbf{S} : \mathbf{S}} \quad \omega = \mathbf{E} \cdot \frac{\mathbf{S} \cdot \left(D_t\mathbf{S}\right) - \left(D_t\mathbf{S}\right) \cdot S}{2\mathbf{S} : \mathbf{S}} \tag{24}$$

where $D_t\mathbf{S}$ is the strain-rate total derivative tensor.

If the curvature correction is not activated, f_c is set to unity. The idea in this approach is to introduce a functional dependence into the eddy viscosity such that the model bifurcates. In rotating and convexly curved flows, the turbulence production decreases. If the rate of rotation or the convex curvature is strong enough, turbulence can no longer be sustained resulting in relaminarization. With the approach proposed by Arolla and Durbin (2013) this effect is created directly by adjusting the eddy viscosity.

2.2 Dynamic Smagorinsky-Lilly model

Recalling Eq. (5), in order to close the set of equations for the LES formulation, one needs to determine C_s. The methodology proposed by Lilly (1992) to improve Germano's model (Germano *et al.*, 1991) consists of minimizing the error of an algebraic equation for C_s instead of taking averages as in the original approach.

The test-to-grid filter length ratio $\hat{L}/\tilde{L} = 2$ is the optimum value as found by Germano *et al.* (1991). For stability purposes, the values of C_s are clipped using minimum and maximum values, so that $C^2_{s_{\min}} = 0$ and $C^2_{s_{\max}} = 10^6$.

3. RESULTS

The simulations were performed for a rotational Reynolds number $Re_\omega = \omega D_h^2/\nu = 5800$ (with D_h representing the duct hydraulic diameter and ν the fluid kinematic viscosity) and an axial Reynolds number $Re_b = W_b D_h/\nu = 5800$ (W_b is the flow bulk velocity). For the duct walls, no-slip BCs were applied. Periodicity was assumed in the streamwise direction and the flow was driven by a constant mass flow rate. The LES results were obtained with a blended third-order central differencing with second-order upwind method. For the SST-based calculations, second-order upwinding was employed. The temporal terms were treated with second-order fully-implicit discretization. The flow statistics were collected for 128 flow-through times. For the SST-based calculations, the simulation was carried out until reaching steady state.

Table 1: Numerical and grid characteristics

	$H^* = h/D_h$	$R[m]$	N_r,N_θ,N_z	$\Delta r_i^+(\Delta r_o^+)$	$\Delta\theta_0^+(\Delta\theta_\alpha^+)$	$\delta t[s]$	CFL_{max}	FTT
LES-DynSMG	4	2	45, 45, 45	0.8187 (0.7511)	0.7877 (0.8106)	0.050	0.160	128
SSTKO	2	2	45, 45, 20	0.4531 (0.3597)	0.4516 (0.4459)	0.10	0.231	-
SSTKO-CC	2	2	45, 45, 20	0.5417 (0.4131)	0.5331 (0.5196)	0.10	0.301	-

Table 1 summarizes the numerical details for both LES and SST simulations. The duct height $H^* = h/D_h$, outer radius R, grid elements in the r-, θ- and z-directions, time-step and respective CFL_{max} are listed for every model. The grid elements were hyperbolically spaced in the wall-normal directions and uniformly spaced in the axial direction.

The problem geometry combined with the rotating frame of reference configure a tremendous challenge to RANS scalar models. Besides rotation-induced phenomena, the model has to account for turbulence production decrease (increase) in convexly (concavely) curved surfaces as well as anisotropy effects due to the corners. Each one of these effects are usually incorporated into the turbulent kinetic energy production term, P_k, in Eq. (11). Although non-linear relations for the eddy viscosity equation have been proposed (Spalart, 2000; Hellsten, 2005; Wallin and Johansson, 2000), in the present study, only curvature and rotation effects are considered.

Figure 2 illustrates the mean axial velocity profile, evaluated at the duct centre plane ($\theta = 0.5\alpha$). The profile magnitudes were normalised by the flow bulk velocity W_b. In Fig. 2a, the solution for the stationary case, in which Re_ω is set to zero, shows two drawbacks of the pure SSTKO model. First, the rotating and non-rotating cases deliver overlapping profiles as an outcome of rotation effects not being captured by scalar eddy viscosity models. Second, the SSTKO profiles are overpredicted when compared with results obtained from the LES solution for the exact same setup. This is related to the fact that linear eddy viscosity models do not account for anisotropy in the Reynolds stress tensor. The Reynolds stresses imbalance causes a secondary motion to develop, draining momentum from the mean flow towards the duct corners and therefore, reducing the axial velocity magnitude at the centre plane. Results were compared with the DNS study of Pinelli *et al.* (2010), where the same phenomenon was reported, showing good agreement between LES and reference DNS results.

The rotation effect, displayed in Fig. 2b, is evidenced as the velocity magnitude is increased. In the flow bulk region, where the main rotating core develops as an outcome of the Coriolis effect, turbulent intensity is reduced due to the stabilising nature of rotation. The SSTKO-CC model is able to mimic this phenomenon and by damping turbulent viscosity, the velocity profile is adjusted, becoming very close to the LES solution. The slight difference found between the profile and also between Figs. 3a and 3c may be a result the presence of the secondary motion, misrepresented by the SSTKO-CC model, which acts redistributing momentum across the duct.

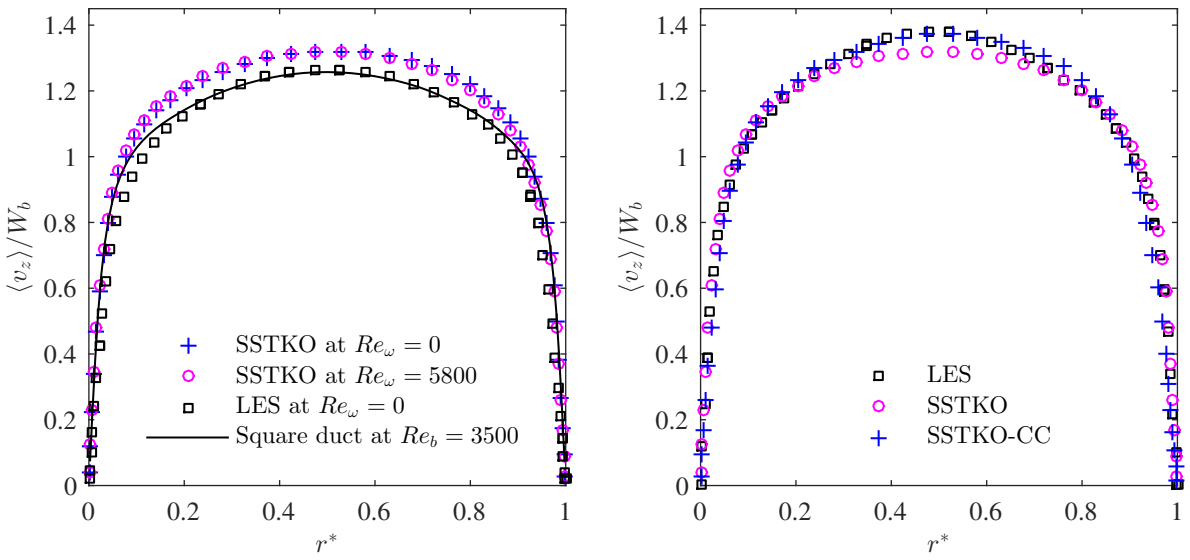

(a) Comparison of SSTKO at $Re_\omega = 0$ and SSTKO at $Re_\omega = 5800$ with LES results at $Re_\omega = 0$ and reference DNS data

(b) Comparison of SSTKO, SSTKO-CC and LES results at $Re_\omega = 5800$

Figure 2: Mean axial velocity profile evaluated at $\theta = 0.5\alpha$. The velocity magnitude was normalised by the flow bulk velocity. Results are compared with the DNS study of Pinelli *et al.* (2010)

Figure 3 displays the mean axial velocity field. In Fig. 3a, obtained from LES results, one can note that some symmetry

is hardly observed. Part of the distortion can be attributed to secondary motion resulting from Coriolis and anisotropy effects. Another part can be attributed to the unbalance in turbulence production in both concave and convex surfaces. The SSTKO model, as in Fig. 3b, is completely blind to these effects, delivering a stationary-like solution. The SSTKO-CC model, on the other hand, provided a reasonable solution qualitatively similar to that obtained from LES.

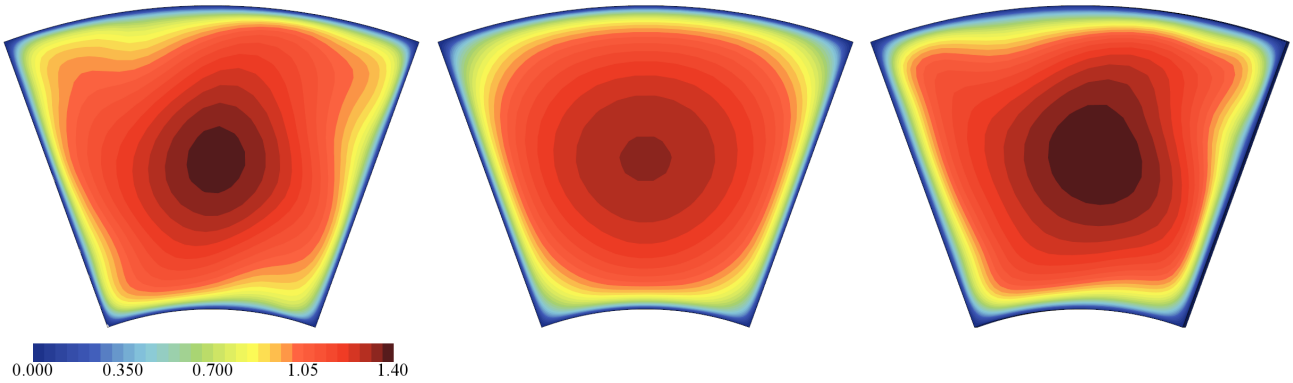

(a) LES-DynSMG (b) SSTKO (c) SSTKO-CC

Figure 3: Mean axial velocity field obtained with the (a) LES DynSMG model (b) SSTKO and (c) SSTKO with curvature correction. The velocity magnitude was normalised by the flow bulk velocity. Rotation direction is clockwise.

Table 2 compares the friction factor value (see Eq.(25)) obtained for both stationary and rotating cases. For $Re_\omega = 0$, the f value, obtained from the experimental correlation $f = 0.2685 Re_b^{-0.25}$ reported in the study of Tao *et al.* (2000) is brought in for comparison. The LES solution agreed very well with the experimental prevision, with a difference of only 0.84%. Between SSTKO and LES solutions, the difference was found to be of 11.02%. The influence of rotation is to increase the value of f, for this case, in about 25% according to the present LES. As seen in Tab. 2, as expected, the SSTKO model is shown to be insensitive to rotational effects. For the SSTKO-CC model, the outcome was not as expected. Instead of increasing the wall shear stress in order to correct the friction factor, the predicted value was off by -28% when compared to the present LES.

Table 2: Friction factor found for both stationary and rotating cases

	$Re_\omega = 0$			$Re_\omega = 5800$		
	LES	SSTKO	Tao *et al.* (2000)	LES	SSTKO	SSTKO-CC
Friction factor $f \times 10^2$	3.104	3.446	3.078	3.881	3.446	2.779

$$f = \frac{-d\overline{P}/dz}{0.5\rho W_b^2} D_h \tag{25}$$

It seems that dumping the turbulent viscosity to account for rotation had a side effect on the viscous stress acting on the walls. In Fig. 4, the turbulent kinetic energy field predicted by the SSTKO, Fig. 4a, and SSTKO-CC, Fig. 4b, are compared. When curvature correction is activated, the predicted turbulent kinetic energy is dumped by one order of magnitude. Since both molecular and turbulent viscosities are considered in the shear stress, an underpredicted value for the SSTKO-CC model is expected.

4. CONCLUSIONS

In this study, the SST variant of the $k-\omega$ turbulence model was evaluated by predicting the Newtonian incompressible turbulent flow for an annular-sector duct, for which solutions were obtained for both stationary and rotating cases. The plain SST model, as expected, was found to be insensitive to rotational effects, providing the exact same solution for both stationary and rotating ducts. When sensitised to curvature and rotation effects, the velocity field was better predicted becoming qualitatively similar to the LES solution. The friction factor for the SSTKO-CC model, however, was unexpectedly worsened when compared to the pure SSTKO, which was associated with the underprediction of the entire turbulent kinetic energy field.

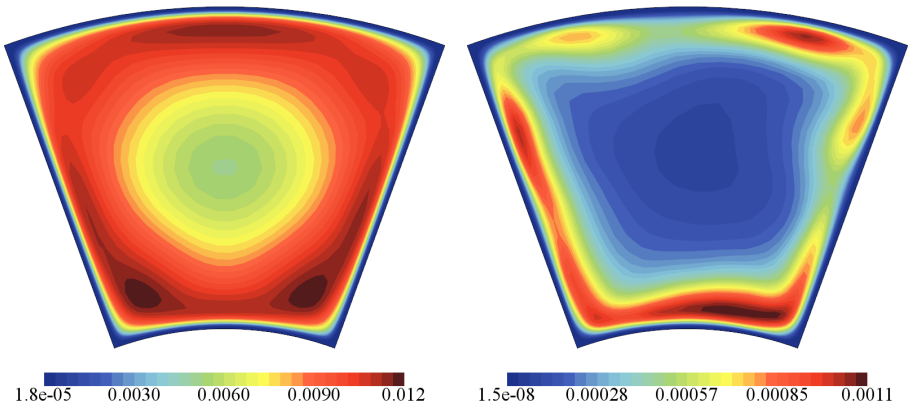

(a) SSTKO (b) SSTKO-CC

Figure 4: Turbulent kinetic energy scalar field obtained with the (a) SSTKO and (b) SSTKO with curvature correction. The magnitude was normalised by the flow bulk velocity. Rotation direction is clockwise.

5. REFERENCES

Arolla, S.K. and Durbin, P.A., 2013. "Modeling rotation and curvature effects within scalar eddy viscosity model framework". *International Journal of Heat and Fluid Flow*, Vol. 39, pp. 78–89.

Durbin, P., 2011. "Review: Adapting Scalar Turbulence Closure Models for Rotation and Curvature". *Journal of Fluids Engineering*, Vol. 133, No. 6, p. 061205. ISSN 00982202. doi:10.1115/1.4004150.

Germano, M., Piomelli, U., Moin, P. and Cabot, W.H., 1991. "A dynamic subgrid-scale eddy viscosity model". *Physics of Fluids A: Fluid Dynamics*, Vol. 3, No. 7, pp. 1760–1765.

Hellsten, A.K., 2005. "New advanced kw turbulence model for high-lift aerodynamics". *AIAA journal*, Vol. 43, No. 9, pp. 1857–1869.

Lilly, D.K., 1992. "A proposed modification of the germano subgrid-scale closure method". *Physics of Fluids A: Fluid Dynamics*, Vol. 4, No. 3, pp. 633–635.

Menter, F.R., 1992. "Improved two-equation k-omega turbulence models for aerodynamic flows".

Menter, F.R., Kuntz, M. and Langtry, R., 2003. "Ten years of industrial experience with the sst turbulence model". *Turbulence, heat and mass transfer*, Vol. 4, No. 1, pp. 625–632.

Patankar, S.V., Pratap, V. and Spalding, D., 1975. "Prediction of turbulent flow in curved pipes". *Journal of Fluid Mechanics*, Vol. 67, No. 03, pp. 583–595.

Pinelli, A., Uhlmann, M., Sekimoto, A. and Kawahara, G., 2010. "Reynolds number dependence of mean flow structure in square duct turbulence". *Journal of fluid mechanics*, Vol. 644, pp. 107–122.

Siemens, P., 2017. "STAR-CCM+ UserâĂŹs Manual".

Smirnov, P.E. and Menter, F.R., 2009. "Sensitization of the sst turbulence model to rotation and curvature by applying the spalart–shur correction term". *Journal of Turbomachinery*, Vol. 131, No. 4, p. 041010.

Spalart, P.R., 2000. "Strategies for turbulence modelling and simulations". *International Journal of Heat and Fluid Flow*, Vol. 21, No. 3, pp. 252–263.

Spalart, P. and Shur, M., 1997. "On the sensitization of turbulence models to rotation and curvature". *Aerospace Science and Technology*, Vol. 1, No. 5, pp. 297–302.

Tao, W.Q., Lu, S.S., Kang, H. and Lin, M., 2000. "Experimental study on developing and fully developed fluid flow and heat transfer in annular-sector ducts". *Journal of Enhanced Heat Transfer*, Vol. 7, No. 1.

Wallin, S. and Johansson, A.V., 2000. "An explicit algebraic reynolds stress model for incompressible and compressible turbulent flows". *Journal of Fluid Mechanics*, Vol. 403, pp. 89–132.

Wilcox, D.C., 1988. "Reassessment of the scale-determining equation for advanced turbulence models". *AIAA journal*, Vol. 26, No. 11, pp. 1299–1310.

6. RESPONSIBILITY NOTICE

The author(s) is (are) the only responsible for the printed material included in this paper.